Unified Analysis of Internal Flowfield in an Integrated Rocket Ramjet Engine. II: Ramjet Sustainer

Hong-Gye Sung[1] and Vigor Yang[2]

Abstract: The flow and combustion dynamics in the ramjet sustainer of an integrated rocket-ramjet (IRR) engine are investigated systematically. The physical model includes the entire engine flowpath, from the freestream in front of the inlet to the exit of the exhaust nozzle. The flowfield obtained previously is used as the initial condition for the present analysis, so that the complete operation history of the engine can be obtained. Various physiochemical processes dictating the engine internal flow development and flame behavior are examined. Emphasis is placed on the interactions between the inlet and combustion dynamics, as well as the overall engine performance. The key mechanisms for driving and sustaining the flow oscillations are explored. In addition, the acoustic wave structures in the engine flowpath are identified.
DOI: 10.1061/(ASCE)AS.1943-5525.0000256.

Author keywords: Integrated rocket-ramjet engine; Ramjet engine; Supersonic inlet aerodynamics; Combustion dynamics.

Introduction

The present work extends from the companion paper Sung and Yang (2014), which deals with the transition from the rocket booster to the ramjet sustainer of an integrated rocket ramjet (IRR) engine to treat the internal flow evolution in the ramjet sustainer. Emphasis is placed on the interactions between the inlet and combustor dynamics, as well as the overall engine performance. The physical domain of concern includes the entire engine flowpath, from the freestream in front of the inlet, through the combustor, to the exit of the exhaust nozzle. The flowfield obtained from Sung and Yang (2014) is used as the initial condition for the present analysis, so that the complete operation history of the IRR engine can be obtained.

The major requirement for ramjet engine design is to achieve efficient and stable operation of the inlet and combustor. The inlet must capture and supply airflow at a rate demanded by the combustor and provide an appropriate stability margin with high pressure recovery (Oh et al. 2005). The combustor must provide robust ignition and smoothly consistent combustion with high efficiency. Despite extensive efforts made over the last five decades, however, realization of those design goals still remains a major technical challenge in the development of a new engine. The major obstacle lies in the difficulty of achieving smooth combustion at various stages of engine operation at a minimum expense of internal flow losses. The intrinsic flow unsteadiness during the transition from the rocket booster to the ramjet sustainer phase often leads to large-amplitude disturbances in the engine flowpath. These disturbances, if not convected or dissipated out efficiently, may give rise to severe oscillations in the combustion chamber. In extreme cases, the acoustic waves induced by unsteady combustion may force the terminal shock wave out of the inlet diffuser and cause a catastrophic failure of the engine.

Because the inlet and combustor are directly coupled, their interactions often exacerbate the flow oscillations in the engine. Typically, the unsteady combustion in the dump chamber generates acoustic waves propagating both upstream and downstream. The upstream-running wave then causes the shock wave in the inlet diffuser to oscillate periodically. This process, in turn, produces disturbances traveling or convecting downstream in the form of an acoustic or entropy wave, which subsequently reinforces the combustion oscillation in the flame zone (Yang and Culick 1986; Sung and Yang 2014). A feedback loop is thus formed for driving and sustaining flow oscillations in the engine. The instability frequencies typically correspond to the frequencies of the natural acoustic modes of the combustor (Crump et al. 1986). The inlet flowfield plays only a minor role in determining the oscillation frequencies, because of the damping of acoustic energy by the terminal shock wave, which acts as an effective absorber for disturbances arising from the downstream region (Culick and Rogers 1983; Oh et al. 2005; Yang and Culick 1985). There are, however, cases in which the instability mechanism is not purely acoustic, but is also associated with large-scale flame motion driven by the periodic vortex shedding at the dump plane (Yu et al. 1991). The vortex shedding frequency is closely related to the flow condition and geometrical configuration in the engine flowpath. It is therefore important to take into account the internal flow development in the entire engine, to faithfully describe the system dynamics.

The purpose of this work is to explore the detailed flow development and combustion dynamics in the ramjet sustainer phase of an IRR engine. The evolution of the flow from the ignition of fresh reactants to stationary operation of the ramjet engine is examined systematically. Results obtained can also be used to facilitate the development of active control of flow and combustion dynamics in ramjet engines (Fung et al. 1991; Fung and Yang 1992)

Ignition Transient

As described in Sung and Yang (2014), the inlet port cover is removed at $t = 0$ ms. Fuel is injected into the ram airflow through an

[1]Professor, School of Aerospace and Mechanical Engineering, Korea Aerospace Univ., Geonggi 200-1, South Korea.

[2]Professor, School of Aerospace Engineering, Georgia Institute of Technology, Atlanta, GA 30332-0150 (corresponding author). E-mail: vigor@gatech.edu

Note. This manuscript was submitted on November 18, 2011; approved on May 15, 2012; published online on May 18, 2012. Discussion period open until August 1, 2014; separate discussions must be submitted for individual papers. This paper is part of the ***Journal of Aerospace Engineering***, Vol. 27, No. 2, March 1, 2014. ©ASCE, ISSN 0893-1321/2014/2-398–403/$25.00.

J. Aerosp. Eng. 2014.27:398-403.

array of choked injectors located 4 cm upstream of the dump plane. The fuel mass flow rate of 0.12 kg/s amounts to an overall equivalence ratio of 0.8. A heat source is supplied in the corner recirculation region downstream of the dump plane and ignition occurs at $t = 2.5$ ms.

To determine the primary factors governing flame propagation, it is valuable to estimate the flame speed based on semiempirical theory. The flame speed depends on the local temperature, pressure, equivalence ratio, turbulence level, and convective velocity. To obtain a maximum possible flame speed, it is assumed that the fuel is mixed completely and that the fuel/air mixture temperature in the combustor is the same as that of the compressed ram air. Meghalchi and Keck (1982) correlated measured laminar-flame speeds, S_L, as follows:

$$S_L(T_u, p) = \left[B_M + B_2\left(\phi - \phi_{M_{\text{ref}}}\right)^2\right]\left(T_u/T_{u_{\text{ref}}}\right)^{\gamma}\left(p/p_{\text{ref}}\right)^{\beta} \quad (1)$$

where $\gamma = 2.18 - 0.8(\phi - 1)$ and $\beta = -0.16 + 0.22(\phi - 1)$. The constants B_M (34.22 cm/s) and B_2 (−138.65 cm/s) were empirically derived. The equivalence ratio, temperature, and pressure are denoted by ϕ, T, and p, respectively. The subscripts u and L represent the unburned mixture property and laminar condition, respectively. For the present chamber condition ($p = 557.29$ kPa; $T = 540$ K; and $\phi = 0.8$), the laminar flame speed is 0.44 m/s. The Klimov model (Klimov 1983) is then applied to predict the turbulent flame speed S_t, because the turbulent fluctuation velocity (v'_{rms}) is much greater than the laminar flame speed in this study

$$S_t/S_L = 3.5\left(v'_{rms}/S_L\right)^{0.7} \quad (2)$$

This yields a value of about 34.3 m/s for the turbulent flame speed. The time required for the flame to reach the nozzle from the ignition location is thus expected to be about 12 ms, in contrast to the numerical result of around 1 ms (see Fig. 14 in Sung and Yang 2014). This difference can be reconciled by considering the transport of thermal energy by the mean flow at a velocity of around 300 m/s, which yields a flame propagation time of around 1.2 ms from the ignition site to the nozzle entrance. The result suggests that the flame propagation is not dominated by turbulent diffusion but instead by the mean flow convection. The influence of the mean flow on flame propagation diminishes in the later stage of the ignition transient, as the mean flow velocity decreases rapidly after the terminal shock in the inlet is established and reaches a stationary condition (Sung and Yang 2014).

Fig. 1 shows the development of the temperature field in the combustor soon after ignition is achieved. The corresponding pressure evolution is given in Fig. 4 of Sung and Yang (2014). The flame propagates along the surface with an optimal local equivalence ratio, which varies continuously because of the vorticies in the shear layer. The flame bulges outward in the radial direction at $t = 4.48$ ms and is stretched downstream axially at $t = 4.71$ ms. It then begins to roll up near the corner of the backward-facing step under the influence of the vortical flow motion at $t = 5.19$ ms. As the roll-up continues downstream, the flame front propagates radially inward at $t = 5.53$ ms and is grossly stretched, so that part of the fresh fuel/air mixture in the leading region is stripped off at $t = 6.02$ ms. Shortly after this, the flame returns to a configuration similar to that at $t = 4.23$ ms. As a consequence of the flame oscillation, the temperature field becomes more uniform in the entire chamber. The flame dynamics is closely coupled with the vortical flow development. The large density gradient caused by the heat release in the flame zone leads to the baroclinic generation of vorticity, which then results in the wrinkling of the flame front.

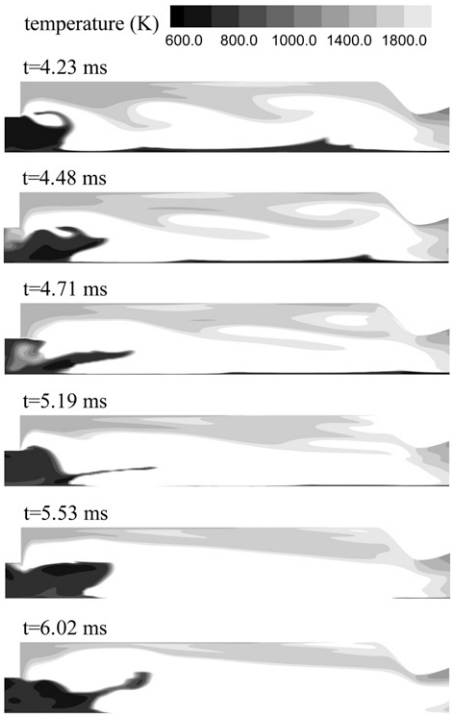

Fig. 1. Temporal evolution of temperature field in combustor during ignition transient

Fig. 2 shows a snapshot of the vorticity field in the entire engine during the ignition transient. A positive value corresponds to counterclockwise motion. Strong vorticies form along the inlet walls, especially on the cowl side, to satisfy the no-slip condition. The flow separation caused by the shock/boundary layer interaction, as well as the flow divergence in the downstream region of the center body, also contribute to the generation of vorticity. In addition, vorticity is produced in the combustion chamber because of the flame motion and the nonuniformity of the velocity field. The large-scale vorticies fluctuate at a time scale commensurate with that of the flame fluttering.

The terminal shock has a strong influence on the wall boundary layers in the inlet. Once the shock is disturbed by the incident acoustic wave originating from the combustor, a vorticity wave arises and is convected downstream. Such a perturbation creates a transverse, wave-like disturbance similar to Tollmien-Schlichting waves transported into turbulent vorticies. After these vortices propagate into the combustion chamber, a large ring vortex forms at the dump plane, if it's shedding frequency matches the frequency of the acoustic wave in the chamber. The formation of this vortex roughly coincides with the temporal maximization of the local pressure. In other words, the large ring vortex is generated at about $t = 5.53$ s, the instant when the acoustic pressure reaches its maximum at the dump plane [see Fig. 4(b) in Sung and Yang 2014]. The vortex shedding frequency can be correlated with the Strouhal number, which has a value of 0.21 based on the height of the dump combustor plane for high-Reynolds-number ($10^3 < \mathrm{R} < 10^7$) flows (White 1986). In the present case, the mean flow velocity is about 250 m/s. The previous correlation gives a shedding frequency of 770 Hz, which is in good agreement with the value of 700 Hz calculated in this study. The large-scale vortical structures have a dominant influence on the flame dynamics and play a pivotal role in driving combustion instability, as pointed out in previous studies (Ahn et al. 2004; Annaswamy and Ghoneim 2002; Barber et al. 2009; Crump et al. 1986; Matveev and Culick 2003; Yu et al. 1991).

J. Aerosp. Eng. 2014.27:398-403.

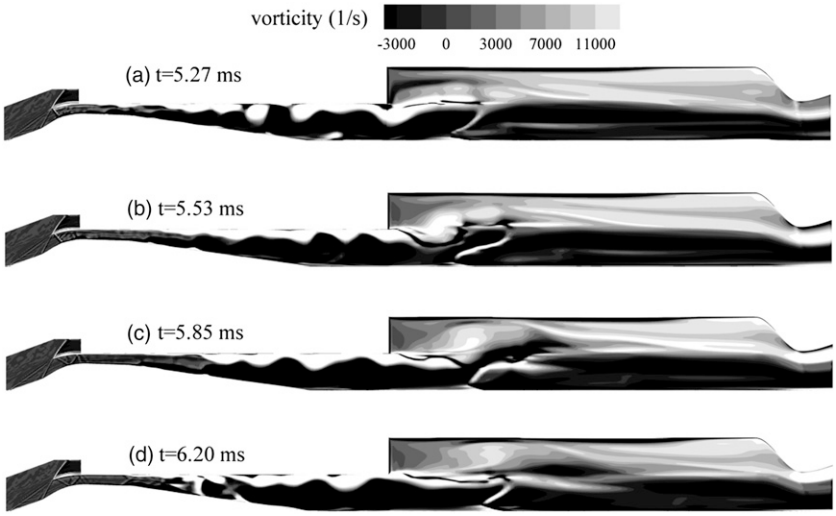

Fig. 2. Temporal evolution of vorticity field in entire engine during ignition transient

Ramjet Operation

After the ignition transient, the chamber pressure levels off at its designed value of 5.5 atm with a finite-amplitude oscillation, as indicated in Fig. 4 of Sung and Yang (2014). Fig. 3 shows the temporal evolution of the temperature field in the combustor within one cycle of oscillation at steady operation. The phase angle θ is in reference to the negative-to-positive zero-crossing pressure immediately downstream of the dump plane. Despite its spatial variation, the temperature field appears to be more uniform than its counterpart during the ignition transient. Fig. 4 shows snapshots of the vorticity, temperature, and Mach number fields in the entire engine at $\theta = \pi$.

The frequency content of flow oscillations at various locations in the engine is examined to provide direct insight into the characteristics of unsteady motions. Fig. 5 shows the power spectrum density of the pressure fluctuation in the combustor. The measurement was made at the corner immediately downstream of the dump plane. The dominant frequencies are 380, 700, and 1,390 Hz, corresponding, respectively, to the bulk, first longitudinal, and second longitudinal modes of the acoustic motion in the chamber. In addition, several higher harmonics were observed with much lower amplitudes. The special structures and the mechanisms responsible for driving and sustaining these modes will be discussed in a later part of this paper.

Fig. 6 shows the temporal evolution of the inlet flowfield within one cycle of oscillation, where TS denotes the terminal shock. The time of each snapshot corresponds to those in Fig. 3. The location of the terminal shock oscillates in response to the periodic pressure fluctuations in the combustor, but with a phase lag. A mechanistic discussion of the shock dynamics and its interaction with the acoustic waves originating from the combustor can be found in the work of Oh et al. (2005). The displacement of the terminal shock (Δx_s) subject to periodic acoustic excitation from the downstream region can be estimated by the following analytical formula, which was developed by Culick and Rogers (1983), based on a one-dimensional inviscid-flow theory:

$$\Delta x_s = \frac{\Delta p}{\overline{p}_1} \times \frac{1}{\sqrt{\left[\frac{2\pi f}{\overline{a}_1} \times \frac{4\gamma \overline{M}_1}{\gamma+1}\right]^2 + \left[\left(\frac{1}{A}\frac{dA}{dx}\right)_s g(\overline{M}_1)\right]^2}} \tag{3}$$

where $\overline{p}_1$, $\overline{a}_1$, and $\overline{M}_1$ = mean pressure, sound speed, and Mach number immediately upstream of the shock, respectively;

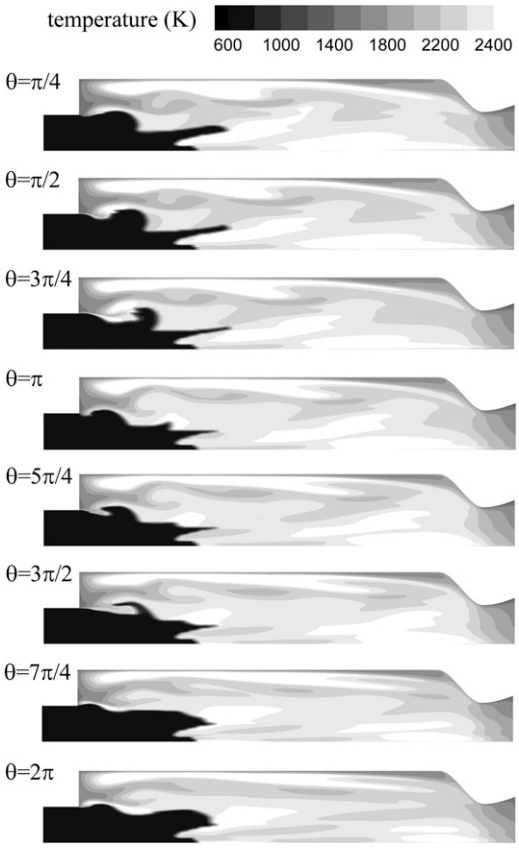

Fig. 3. Temporal evolution of temperature field in combustor within one cycle of oscillation during ramjet operation, $f = 380\,\text{Hz}$

Δp = amplitude of the pressure oscillation behind the shock; and A = cross-sectional area. The subscript s represents the value at the normal shock and

$$g(\overline{M}_1) = \frac{(\gamma^2+1)\overline{M}_1^2 + (\gamma-1)}{(\gamma+1)^2/2\gamma} \tag{4}$$

Fig. 7 shows a comparison of the shock displacement predicted by the present analysis and the analytical formula. The amplitude of

J. Aerosp. Eng. 2014.27:398-403.

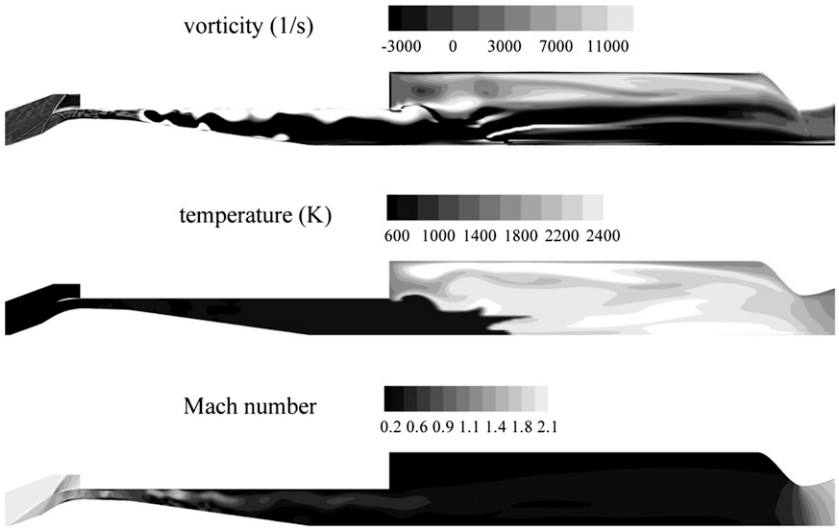

Fig. 4. Snapshots of vorticity, temperature, and Mach number fields over entire engine at $\theta = \pi$

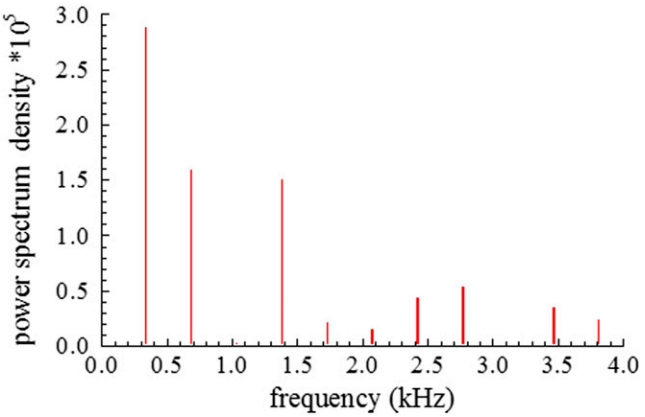

Fig. 5. Frequency spectrum of pressure fluctuation at combustor corner immediately downstream of dump plane

the pressure oscillation Δp used in the theoretical calculation is 5% of the mean pressure. The shock displacement decreases rapidly with increasing frequency of the oscillation. The theory overpredicts the displacement, mainly because of the neglect of viscous boundary layer and multidimensional effects. Furthermore, the theory only treats a simple sinusoidal oscillation at 380 Hz, whereas many harmonics exist in the numerical result, as evidenced in the frequency spectrum shown in Fig. 5.

The spatial distribution of the oscillating field is examined to identify the acoustic wave properties over the entire engine flowpath. Figs. 8 and 9 show the amplitude and phase distributions of pressure oscillations for the 380- and 700-Hz modes, respectively. The data were obtained from spectral analysis of the calculated pressure oscillations along the midway of the flow path. The fluctuating pressure is normalized with respect to its local time-mean quantity, and the phase angle is in reference to the value at the dump plane.

For the case of $f = 380$ Hz (i.e., the first harmonic in the frequency spectrum shown in Fig. 5), the uniform distribution of the phase angle in the combustor suggests the existence of a bulk mode in the chamber. The acoustic field in the inlet is dominated by an upstream-running wave originating from the combustor.

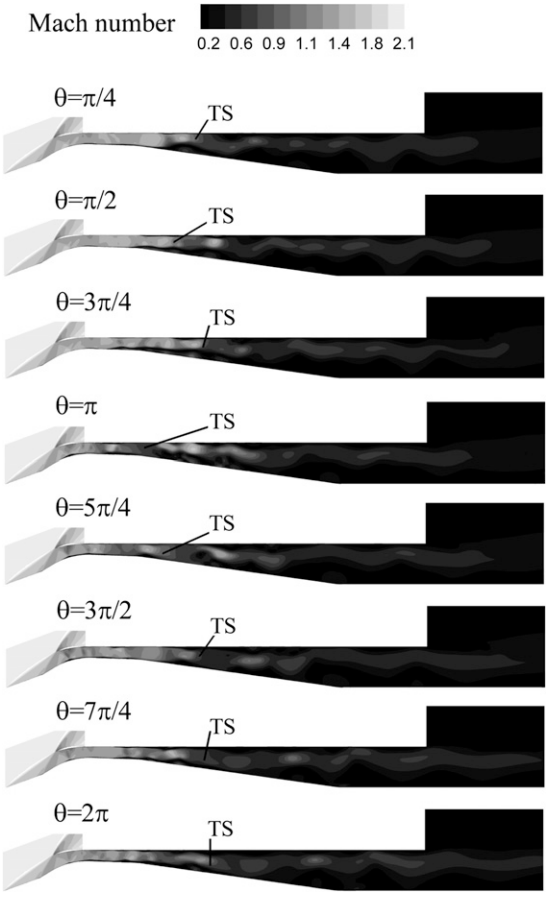

Fig. 6. Temporal evolution of inlet flowfield within one cycle of oscillation during ramjet operation, $f = 380$ Hz (TS = terminal shock)

The terminal shock acts as a damper that can effectively absorb the energy of the incident wave from the downstream region (Crump et al. 1986; Culick and Rogers 1983; Oh et al. 2005; Yang and Culick 1985). Consequently, the acoustic wave reflected from the terminal shock becomes very weak. The constant amplitude of

J. Aerosp. Eng. 2014.27:398-403.

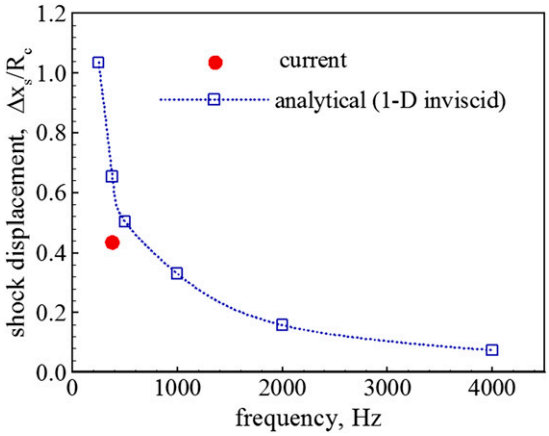

Fig. 7. Comparison of shock displacement predicted by the present analysis and analytical formula: R_c = cowl height of the intake [shown in Fig. 2(a) of Sung and Yang 2014]

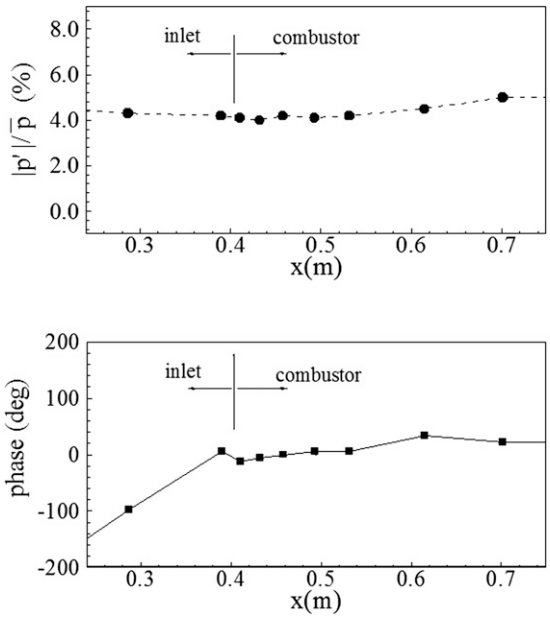

Fig. 8. Distribution of normalized amplitude and phase of pressure oscillation along the midway of the flow path, $f = 380$ Hz

pressure oscillation in the inlet further corroborates the prevalence of the traveling acoustic wave in the inlet.

The situation for the case of $f = 700$ Hz (i.e., the second mode shown in Fig. 5) is considerably different. The oscillatory field in the combustor exhibits a structure of the first longitudinal mode. A pressure nodal point is present in the middle of the chamber, across which a phase difference of 180° occurs. As in the 380-Hz mode, an upstream-running acoustic wave prevails in the inlet with an almost linear distribution of the phase angle. The large pressure fluctuation in the inlet mainly arises from the shock motion and its subsequent effect on the boundary layer, as shown in Fig. 6. The wavelength of the acoustic motion may also be reduced because of the relatively high Mach number (around 0.3) in the inlet (Crump et al. 1986).

The interaction between the terminal shock and combustion chamber dynamics can be explored by applying a spectral analysis as follows:

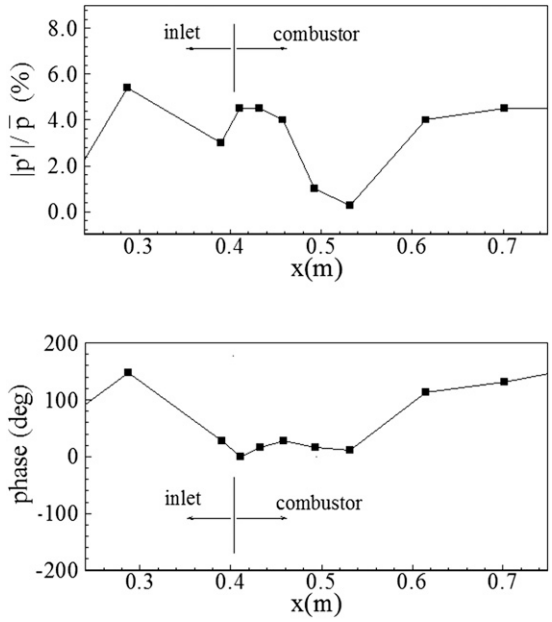

Fig. 9. Distribution of normalized amplitude and phase of pressure oscillation along the midway of the flow path, $f = 700$ Hz

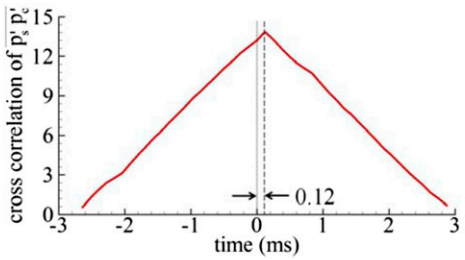

(a) Cross correlation between p'_s and p'_c

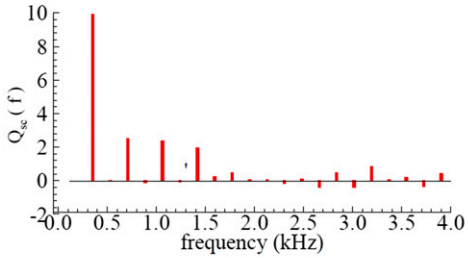

(b) Imaginary part of PSD of cross-correlation between p'_s and p'_c

Fig. 10. Cross-spectral analysis of pressure fluctuations immediately downstream of the terminal shock wave and dump plane: (a) cross-correlation between p'_z and p'_c; (b) imaginary part of power spectral density (PSD) of cross-correlation between p'_z and p'_c

$$S_{xy}(f) = \int_{-\infty}^{\infty} R_{xy}(\tau) e^{-i2\pi f\tau} d\tau = |S_{xy}(f)| e^{-i\theta_{xy}(f)} = C_{xy}(f) - iQ_{xy}(f) \quad (5)$$

where S_{xy} and R_{xy} = two-sided, cross-spectral density function and cross-correlation of signals x and y, respectively; and f and θ = frequency and phase angle, respectively. The signs of $C_{xy}(f)$ and

J. Aerosp. Eng. 2014.27:398-403.

$Q_{xy}(f)$ may be either positive or negative; the sign gives the quadrant for the phase angle. These signs also determine whether $y(t)$ leads $x(t)$ or vice versa at each frequency. Fig. 10(a) shows a cross-correlation of the pressure fluctuations at locations immediately downstream of the terminal shock and dump plane, denoted by the subscripts s and c, respectively. The terminal shock is clearly shown to be driven by the pressure oscillations in the combustor. The time lag of 0.12 ms at the maximum value of the cross-correlation amounts to the time required for the acoustic wave to travel from the dump plane to the terminal shock. Fig. 10(b) presents the imaginary part of the cross-spectral density function. The positive value of $Q_{sc}(f)$ in the frequency range of 0–2 kHz indicates that the pressure oscillation in the combustor leads the shock wave motion. This further corroborates the fact that unsteady combustion in the chamber generates periodic excitations in the form of the bulk and longitudinal modes. The resultant acoustic wave then propagates upstream to induce shock oscillation. On the other hand, the shock motion leads the pressure oscillation in the chamber at certain higher frequencies, as indicated by the negative value of $Q_{sc}(f)$ for $f > 2$ kHz. This phenomenon can be attributed to the flow-induced oscillations in the inlet. The shock/boundary layer interaction and its influence on flow displacement generate disturbances over wide range of frequency spectra.

Summary and Conclusions

A comprehensive analysis was conducted to study the flow and combustion dynamics in the entire flowpath of an IRR engine under ramjet operation. The physical domain of interest extends from the free stream upstream of the inlet entrance through the exhaust nozzle. The flowfield obtained from Sung and Yang (2014) is used as the initial condition, so that the entire operation history of an IRR engine can be explored systematically.

The present work provides detailed information about the interaction between the inlet and combustor dynamics. Various underlying processes responsible for driving and sustaining the flow and combustion instabilities in an IRR engine have been identified. The work starts with an investigation of the evolution of the flow from the ignition of fresh reactants to the stationary state of the ramjet engine. The combustion chamber pressure first experiences a significant overshoot during the ignition process and then levels off at the design condition with a finite-amplitude oscillation. The peak-to-peak magnitude is about 5% of the mean pressure. The oscillatory field is characterized by several well-organized flow motions corresponding to the bulk and longitudinal modes of acoustic waves in the combustor. The unsteady combustion generates acoustic waves propagating upstream and interacting with the inlet flowfield. The resultant shock oscillation and flow variation in the inlet then give rise to fluctuating vortices traveling downstream. A feedback loop is thus established and leads to a large excursion of flow oscillation in the entire engine.

References

Ahn, K., Stamp, G., and Yu, K. H. (2004). "Vortex-heat release interaction in a dump combustor." *Proc., 30th Int. Symp. on Combustion*, Combustion Institute, Pittsburgh, PA, 212–220.

Annaswamy, A. M., and Ghoneim, A. F. (2002). "Active control of combustion instability: Theory and practice." *IEEE Control Syst. Mag.*, 22(6), 37–54.

Barber, T., Maicke, B., and Majdalani, J. (2009). "Current state of high speed propulsion: Gaps, obstacles and technological challenges in hypersonic applications." *AIAA Paper 09-5118, 35th AIAA/ASME/SAE/ASEE Joint Propulsion Conference & Exhibit*, American Institute of Aeronautics and Astronautics (AIAA), Reston, VA.

Crump, J. E., Schadow, K. C., Yang, Y., and Culick, E. C. (1986). "Longitudinal combustion instability in ramjet engines: Identification of acoustic modes." *J. Propul. Power*, 2(2), 105–109.

Culick, E. C., and Rogers, T. (1983). "The response of normal shocks in diffusers." *AIAA J.*, 21(10), 1382–1390.

Fung, Y. T., and Yang, Y. (1992). "Active control of nonlinear pressure oscillation in combustion chambers." *J. Propul. Power*, 8(6), 1282–1289.

Fung, Y. T., Yang, Y., and Sinha, A. (1991). "Active control of combustion instabilities with distributed actuators." *Combust. Sci. Technol.*, 78(4–6), 217–245.

Klimov, A. M. (1983). "Premixed turbulent flames-interplay of hydrodynamic and chemical phenomena." *Prog. Astronaut. Aeronaut.*, 88(2), 133–146.

Matveev, K. I., and Culick, F. E. C. (2003). "A model for combustion instability involving vortex shedding." *Combust. Sci. Technol.*, 175(6), 1059–1083.

Metghalchi, M., and Keck, V. (1982). "Burning velocities of mixtures of air with methanol, isooctane, and indolene at high pressure and temperatures." *Combust. Flame*, 48, 191–210.

Oh, J. Y., Ma, F., Hsieh, S. Y., and Yang, V. (2005). "Interactions between shock and acoustic waves in a supersonic inlet diffuser." *J. Propul. Power*, 21(3), 486–495.

Sung, H.-G., and Yang, V. (2014). "Unified analysis of internal flowfield in an integrated rocket ramjet engine. I: Transition from rocket booster to ramjet sustainer." *J. Aerosp. Eng.*, 10.1061/(ASCE)AS.1943-5525.0000255, 390–397.

White, F. M. (1986). *Fluid mechanics*, 2nd Ed., McGraw Hill, New York.

Yang, V., and Culick, F. E. C. (1985). "Analysis of unsteady inviscid diffuser flow with a shock wave." *J. Propul. Power*, 1(3), 222–228.

Yang, V., and Culick, F. E. C. (1986). "Analysis of low frequency combustion instabilities in a laboratory ramjet combustor." *Combust. Sci. Technol.*, 45(1), 1–25.

Yu, K. H., Trouvé, A., and Daily, J. W. (1991). "Low-frequency pressure oscillations in a model ramjet combustor." *J. Fluid Mech.*, 232, 47–72.

J. Aerosp. Eng. 2014.27:398-403.